Original article

Simulation of washing of packed bed of porous particles using quintic Hermite splines

Shelly Arora [a], František Potuček [b], Inderpreet Kaur [a,*]

[a] Department of Mathematics, Punjabi University, Patiala 147002, Punjab, India
[b] Institute of Chemistry and Technology of Macromolecular Materials, University of Pardubice, Czech Republic

ABSTRACT

A comprehensive two phase non-linear mathematical model has been presented with special reference to particle geometry and pore radius of particles. Model equations have been divided into bulk fluid phase and particle phase. Bulk fluid phase is characterized by external fluid whereas particle phase signifies the intraparticle solute concentration and solute concentration adsorbed on particle surface. Interparticle solute concentration and the concentration of solute adsorbed on particle surface are related by Langmuir adsorption isotherm. Model equations have been discretized numerically by Hermite collocation method with quintic basis. Effect of different parameters has been shown via breakthrough curves. Model predicted values have been compared to experimental values given in literature to check the applicability of the model.

© 2018 The Authors. Production and hosting by Elsevier B.V. on behalf of King Saud University. This is an open access article under the CC BY-NC-ND license (http://creativecommons.org/licenses/by-nc-nd/4.0/).

1. Introduction

Problems of heat and mass transfer during flow through packed bed of porous particles are of great interest for mathematicians as well as engineers. From Brenner (1962) to Arora et al. (2017), number of models have been developed to characterize the fluid flow through packed beds of porous particles.

There exists a chemical system which consists of a single solute flowing through the packed bed and passes through a transient period or for short time period such that sudden changes occur in the influent concentration of the solute. The mechanism is controlled by the rate at which the material in the solute is taken up by the particles in the packed bed (Rosen, 1952). The main motive of the study is to consider a liquid containing a solute moving with a constant linear velocity 'u' through a packed bed of length 'L'. The rate determining factor is the process of solid diffusion in the particles and the delay in the system is introduced by the thin film surrounding the particles. Behaviour of the system during the transient period is determined by diffusion process. During this process, the solute present in the irregular void channels of the bed diffuse out of particle pores. Displacement of solute from these pores is associated with diffusion like dispersion of external fluid in the direction of flow.

Main purpose of the present study is to develop a mathematical model for washing of packed bed of solid and semi solid particles with the help of external fluid passing through the bed. The removal of soluble and insoluble impurities adsorbed on the particle surface with the help of external fluid is called washing. Due to the porous nature of particles, the solute present in intraparticle voids diffuses out when it comes in contact with external fluid. Mass transfer takes place from particle pores to particle surface and then to external fluid (Arora and Potuček, 2009). Present paper is fabricated with six sections starting from introduction. Model for washing of particles is given in second section. The experimental procedure is presented in third section whereas fourth section describes the numerical technique and application to the model. In fifth section the results obtained from the study are summarized and finally the conclusions of present study are given in sixth section.

2. Mathematical model

Number of mathematical models has been developed from the past few decades to study the washing of porous structure of particles. From Brenner (1962) to Arora et al. (2017), different

* Corresponding author.
E-mail addresses: frantisek.potucek@upce.cz (F. Potuček), inder3003@gmail.com (I. Kaur).

Peer review under responsibility of King Saud University.

Nomenclature

Bi	Biot number, dimensionless $(= k_f \beta R / \overline{K} D_F)$
c	concentration of solute in the liquor (kg/m$_3$)
C	dimensionless concentration $(= c/C_0)$
C_0	solute concentration in the vat (kg/m^3)
C_1	dimensionless parameter $(= C_0/C_F)$
Ce	exit solute concentration, dimensionless
C_F	fiber consistency (kg/m^3)
D_F	intrafiber diffusion coefficient (m^2/s)
D_L	axial dispersion coefficient (m^2/s)
$\overline{K}$	volume equilibrium constant, dimensionless
k^*	mass transfer coefficient, dimensionless $(= k_2/k_1)$
k_1, k_2	mass transfer coefficient $(1/s)$
k_f	film mass transfer coefficient (m/s)
L	thickness of packed bed (m)
n	concentration of solute adsorbed on the fibers(kg/m^3)
N	dimensionless concentration of solute adsorbed on fibers$(= n/N_0)$
N_0	initial concentration of solute adsorbed on the fibers(kg/m^3)

N_1	dimensionless parameter $(= \overline{K} N_0/C_0)$
P_1	dimensionless parameter $(= k_1 R^2/D_F)$
Pe	Péclet number, dimensionless $(= uL/D_L)$
Q	dimensionless pore liquid concentration$(= q/C_0)$
q	pore liquid concentration (kg/m^3)
R	fiber radius (m)
r	radial position in particle (m)
t	time(s)
u	interstitial fluid velocity through bed (m/s)
z	distance from point of introduction of solvent (m)
β	particle porosity, dimensionless
ε	porosity of cake, dimensionless
η	dimensionless radial coordinate $(= r/R)$
θ	$2(1-\varepsilon)(\varepsilon)$
ξ	dimensionless axial coordinate $(= z/L)$
τ	dimensionless time $(= tD_F/R^2)$
ψ	dimensionless parameter $(= \overline{K} Ru/k_f \beta L)$.

investigators have developed different models time to time to study the displacement washing of porous particles. Most of them have developed linear models to study the washing process. However, Arora et al. (2006) to Arora et al. (2017) have presented two phase flow of fluid through packed bed of solid particles by a non linear model involving particle diffusion and axial dispersion coefficient. In present study, two phase non linear mathematical model involving particle diffusion, axial dispersion coefficient, pore radius of particles, bed porosity and film resistance mass transfer coefficient has been discussed. Interparticle solute concentration and solute concentration adsorbed on particle surface have been related by Langmuir adsorption isotherm. External fluid concentration is taken to be a function of axial distance and time whereas interparticle solute concentration and solute concentration adsorbed on particle surface have been taken as function of pore radial distance, axial distance and time. In Fig. 1, schematic representation of packed bed is presented whereas the representation of different zones of packed bed is given in Fig. 2. Model equations have been studied under certain assumptions given in Arora et al. (2015). To avoid the complexities of change of temperature, system is assumed to be isothermal. Bed is taken to be macroscopically uniform and particles are assumed to be porous and of uniform size. Axial distance of the bed is comparatively large from particle diameter and length. Movement of solute within particle
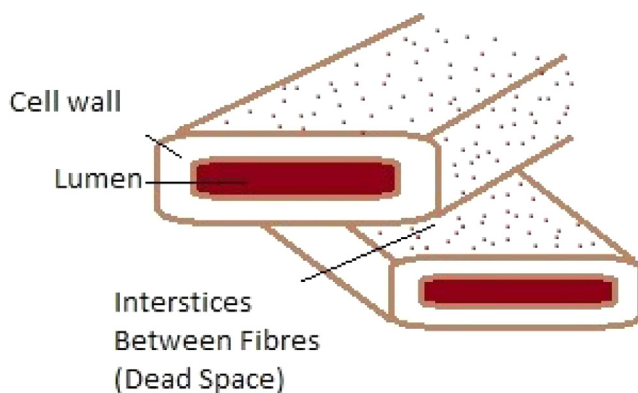
pores is described by Fick's law. Dispersion of solute is defined by axial dispersion coefficient and diffusion in particle pores is described by intraparticle diffusion coefficient. Both are assumed to be independent from axial and radial distances. Two phases of the model have been studied in terms of particle phase and external fluid phase.

2.1. Model for particle phase

Movement of solute through the particle pores is defined by a transient equation mentioned in Arora et al. (2015):

$$\frac{\partial w}{\partial t} = D_F \left(\frac{\partial^2 w}{\partial r^2} + \frac{1}{r} \frac{\partial w}{\partial r} \right) \tag{1}$$

where 'w' is the local intraparticle solute concentration. Since 'w' does not distinguish between intraparticle solute concentration and the solute concentration adsorbed on particle surface, therefore, surface diffusion effects are assumed to be negligible. Transport equation is described by a diffusion equation involving intraparticle solute concentration and solute concentration adsorbed on particle surface. Intraparticle solute concentration

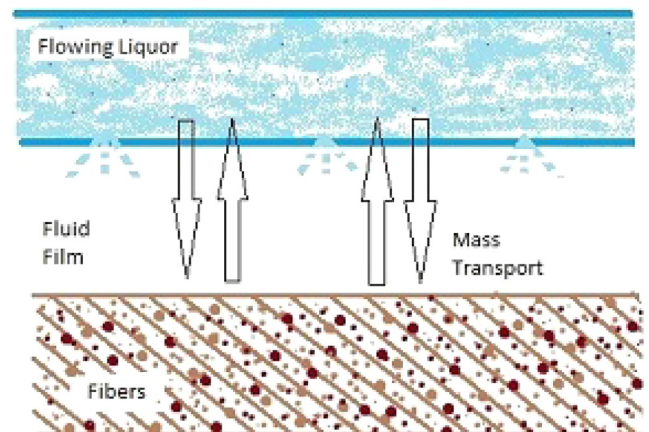Fig. 1. Schematic representation of fibers.

Fig. 2. Schematic representation of different zones.

gradient acts as driving force for diffusion. Therefore, the resulting equation for particle phase is:

$$\frac{\partial q}{\partial t} + \overline{K}\frac{1-\beta}{\beta}\frac{\partial n}{\partial t} = D_F\left(\frac{\partial^2 q}{\partial r^2} + \frac{1}{r}\frac{\partial q}{\partial r}\right) \tag{2}$$

with $w = \beta q + \overline{K}(1-\beta)n$. By assumption, local equilibrium prevails in intraparticle pores.

2.2. Adsorption isotherm

Number of investigators (Brenner, 1962; Sherman, 1964; Pellett, 1966; Potuček, 1997; Arora et al., 2014) have followed linear adsorption isotherm to simplify the mathematical complexities. However, under practical situation intraparticle solute concentration and solute concentration adsorbed on particle surface are related to each other by non linear kinetics. Therefore, these are related by Langmuir kinetics (Arora et al., 2006, 2015) and the following equation is obtained.

$$\frac{\partial n}{\partial t} = k_1\frac{q}{C_F}(N_0 - n) - k_2 n \tag{3}$$

where k_1 and k_2 are deposition and detachment rate constants.

2.3. External fluid phase

Transport phenomenon in the porous media having void fraction ε is described by one dimensional axial dispersion model involving axial dispersion and molecular diffusivity. Since molecular diffusivity is negligible as compared to axial dispersion and is therefore ignored. The model for external fluid is represented by an axial dispersion model given in Arora et al. (2006, 2015) involving accumulation term and dispersion term as follows:

$$D_L\frac{\partial^2 c}{\partial z^2} = u\frac{\partial c}{\partial z} + \frac{\partial c}{\partial t} + \frac{(1-\varepsilon)}{\varepsilon}\frac{\partial \hat{q}}{\partial t} \tag{4}$$

where $\hat{q}$ is defined as the volume average concentration in particles.

Basically, there are two types of rate mechanisms in packed bed of particles. First one describes $\frac{\partial q}{\partial t}$ explicitly in terms of c and q and is already discussed in Arora and Potuček (2009). In second type of rate mechanism, $\hat{q}$ is defined in terms of an integral equation discussed below:

$$\hat{q} = \frac{2}{R^2}\int_0^R q(r,z,t)r\,dr \tag{5}$$

Eq. (4) provides a link between particle phase and external fluid phase. Neretnieks (1974), Raghvan and Ruthven (1983), Arora et al. (2015) have related the particle phase and external fluid phase by defining a condition at particle boundary to obtain the following term:

$$\frac{\partial \hat{q}}{\partial t} = \frac{2k_f\beta}{\overline{K}R}(c - q|_{r=R}) \tag{6}$$

2.4. Initial and boundary conditions

Particle phase model has one boundary condition at center of the particle (at $r = 0$) and the other at the surface of the particle (at $r = R$). By assumption, concentration gradient is taken to be zero at the center of the particle, therefore, a Neumann type condition is obtained, *i.e.*,

$$\frac{\partial q}{\partial r} = 0 \qquad \text{at } r = 0 \tag{7}$$

Transport of solute between particle surface and its surrounding is assumed to take place in a thin film surrounding the particle (Arora

et al. (2006)). On particle surface, there exists external mass transfer resistance k_f due to the diffusion of solute. Transport between the surface of the particle and interior of the particle is a diffusive process. Hence mass balance on the surface of the particle gives:

$$\frac{k_f\beta}{\overline{K}}(q|_{r=R} - c) = -D_F\frac{\partial q}{\partial r} \qquad \text{at } r = R \tag{8}$$

It is assumed that there is no step change in the solute concentration and there will be no loss of solute from the bed through the plane at which the displacing fluid is introduced. Concentration gradient is taken to be zero at the outlet of the bed, to avoid the fact that fluid will pass through the maximum or minimum in the interior of the bed (Brenner, 1962; Arora et al., 2006). Therefore, external fluid phase is subjected to the following boundary conditions at inlet and outlet of the bed, respectively.

$$uc - D_L\frac{\partial c}{\partial z} = 0 \qquad \text{at } z = 0 \tag{9}$$

$$\frac{\partial c}{\partial z} = 0 \qquad \text{at } z = L \tag{10}$$

Initially, it is assumed that intra-particle, inter-particle and bulk fluid concentrations are equal to initial solute concentration.

$$c = q = C_0 \text{ and } n = N_0 \qquad \text{at } t = 0 \tag{11}$$

System of equations from Eq. (2) to Eq. (11), is converted into dimensionless form. The given system of equations is similar to the system of equations discussed in Arora et al. (2015).

$$\frac{\partial^2 Q}{\partial \eta^2} + \frac{1}{\eta}\frac{\partial Q}{\partial \eta} = \frac{\partial Q}{\partial \tau} + \frac{(1-\varepsilon)}{\varepsilon}N_1\frac{\partial N}{\partial \tau} \tag{12}$$

$$\frac{\partial N}{\partial \tau} = P_1(C_1 Q(1-N) - k^*N) \tag{13}$$

$$\frac{\partial C}{\partial \tau} = \frac{\psi Bi}{Pe}\frac{\partial^2 C}{\partial \xi^2} - \psi Bi\frac{\partial C}{\partial \xi} - \theta Bi(C - Q|_{\eta=1}) \tag{14}$$

$$\frac{\partial Q}{\partial \eta} = 0 \qquad \text{at } \eta = 0 \text{ and } \tau > 0 \tag{15}$$

$$\frac{\partial Q}{\partial \eta} = Bi(C - Q|_{\eta=1}) \quad \text{at } \eta = 1 \text{ and } \tau > 0 \tag{16}$$

$$C - \frac{1}{Pe}\frac{\partial C}{\partial \xi} = 0 \quad \text{at } \xi = 0 \text{ and } \tau > 0 \tag{17}$$

$$\frac{\partial C}{\partial \xi} = 0 \qquad \text{at } \xi = 1 \text{ and } \tau > 0 \tag{18}$$

$$C = Q = N = 1 \qquad \forall \xi \in (0,1) \text{ and } \eta \in (0,1) \tag{19}$$

3. Experimental procedure and properties of pulp bed

The stimulus–response experiments, using a step input, have been carried out in the displacement washing cell given in Fig. 3. Details of the washing cell and other experimental apparatus have been described in Potuček (1997). Permeability, Porosity, Interstitial fluid velocity and axial dispersion coefficient have been explained in Arora and Potuček (2009, 2012). Physical properties of pulp bed were determined through experimental output using the parameters given in Table 1.
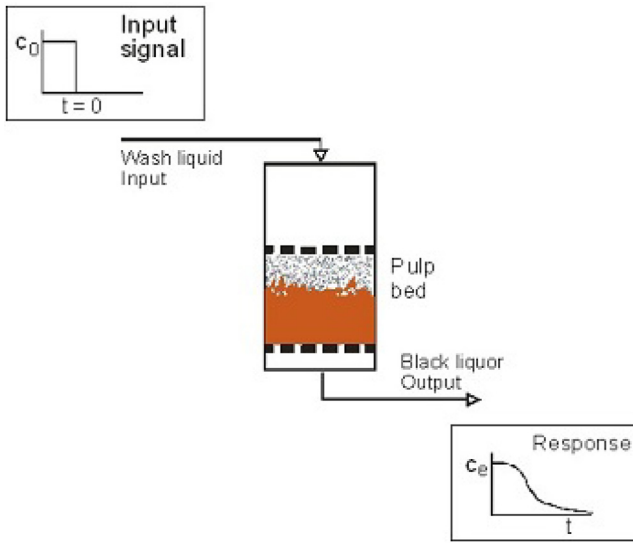
Fig. 3. Schematic representation of the system of washing cell.

Table 1
Experimental values for pulp bed.

Parameter	Value	Unit
Pe	12.25–20.81	–
ε	0.5561–0.8120	–
u	$(1.25–4.23)\times10^{-4}$	m/s
Consistency	7.96–16.60	%
D_L	$(1.816–9.074)\times10^{-7}$	m^2/s
β	0.7246	–

4. Quintic hermite collocation method (QHCM)

Orthogonal collocation is one of the weighted residual methods used to discretize the boundary value problems. It is one of the simplest methods to discretize the boundary value problems. In this method an interpolating polynomial is chosen as a base function to approximate the trial function and then the trial function is adjusted in the given problem to get the residual. The residual is defined over its region and is set equal to zero at collocation points.

Quintic Hermite collocation is one of the collocation techniques in which the base function is chosen to be the quintic Hermite interpolating polynomials. In this technique the trial function is approximated by Hermite interpolating polynomials of order 5. It is the generalization of Lagrange interpolation with polynomials that not only interpolate function at each node point but also its consecutive derivatives. Quintic Hermite interpolating polynomials can be expressed in the following form:

$$\sum_{j=1}^{6} p(\xi_j)P_j(\xi) + p'(\xi_j)\overline{P}_j(\xi) + p''(\xi_j)\overline{\overline{P}}_j(\xi), \tag{20}$$

Details of $P_j(\xi), \overline{P}_j(\xi)$ and $\overline{\overline{P}}_j(\xi)$ can be taken form Arora and Kaur (2018)

Collocation is applied within each sub-domain in radial and axial direction by introducing new variables η^* and ξ^*, respectively in such a way that $\xi^* = \frac{\xi-\xi_\gamma}{h_\gamma}$ where $h_\gamma = \xi_{\gamma+1} - \xi_\gamma, \xi^* = 0$ when $\xi = \xi_\gamma$ and $\xi^* = 1$ when $\xi = \xi_{\gamma+1}$. $\eta^* = \frac{\eta-\eta_\ell}{h_\ell}$ where $h_\ell = \eta_{\ell+1} - \eta_\ell, \eta^* = 0$ when $\eta = \eta_\ell$ and $\eta^* = 1$ when $\eta = \eta_{\ell+1}$. After rearranging the terms $P_j(\xi), \overline{P}_j(\xi)$ and $\overline{\overline{P}}_j(\xi)$ can be written in simplified form as:

$$H_1(\xi^*) = (1 - 10\xi^{*3} + 15\xi^{*4} - 6\xi^{*5})$$

$$H_2(\xi^*) = h_\gamma(\xi^* - 6\xi^{*3} + 8\xi^{*4} - 3\xi^{*5})$$

$$H_3(\xi^*) = h_\gamma^2(0.5\xi^{*2} - 1.5\xi^{*3} + 1.5\xi^{*4} - 0.5\xi^{*5})$$

$$H_4(\xi^*) = h_\gamma^2(0.5\xi^{*3} - \xi^{*4} + 0.5\xi^{*5})$$

$$H_5(\xi^*) = (10\xi^{*3} - 15\xi^{*4} + 6\xi^{*5})$$

$$H_6(\xi^*) = h_\gamma(-4\xi^{*3} + 7\xi^{*4} - 3\xi^{*5}) \tag{21}$$

The symmetry property in quintic Hermite polynomials is also satisfied with $H_1(\xi^*) = H_5(1 - (\xi^*)), H_2(\xi^*) = -H_6(1 - (\xi^*))$ and $H_3(\xi^*) = H_4(1 - (\xi^*))$.

$C^\gamma(\xi^*, \tau)$ is taken to be the approximating function for $C(\xi^*, \tau)$, similarly $Q^{(\ell,\gamma)}(\eta^*, \xi^*, \tau)$ and $N^{(\ell,\gamma)}(\eta^*, \xi^*, \tau)$ have taken as the approximating functions for $Q(\eta^*, \xi^*, \tau)$ and $N(\eta^*, \xi^*, \tau)$, respectively. Approximating functions have been defined as:

$$C^{(\gamma)}(\xi^*, \tau) = \sum_{i=1}^{6} c_i^{(\gamma)} H_i(\xi^*) \tag{22}$$

$$Q^{(\ell,\gamma)}(\eta^*, \xi^*, \tau) = \sum_{i=1}^{6} q_i^{(\ell,\gamma)} H_i(\eta^*) \tag{23}$$

$$N^{(\ell,\gamma)}(\eta^*, \xi^*, \tau) = \sum_{i=1}^{6} n_i^{(\ell,\gamma)} H_i(\eta^*) \tag{24}$$

where c_i, q_i and n_i are continuous functions of τ.

Next step in the collocation technique is the choice of collocation points. In present study zeros of Legendre polynomials have been taken as collocation points in both radial as well as axial direction. Details of method has been given in Arora and Kaur (2016, 2018).

4.1. Application of QHCM

Using the approximation of $Q(\eta, \xi, \tau), N(\eta, \xi, \tau)$ and $C(\xi, \tau)$ given in previous section at j^{th} collocation point in radial direction and k^{th} collocation point in axial direction, following system of equations is obtained:

$$\sum_{i=1}^{6} \frac{dq_i^{(\ell,\gamma)}}{d\tau} H_{ji} = \frac{1}{h_\ell^2} \sum_{i=1}^{6} q_i^{(\ell,\gamma)} B_{ji} + \frac{1}{(\eta_j^* h_\ell + \eta_\ell)h_\ell} \sum_{i=1}^{6} q_i^{(\ell,\gamma)} A_{ji}$$
$$- \frac{(1-\varepsilon)}{\varepsilon} N_1 P_1 \left(C_1 \left(\sum_{i=1}^{6} q_i^{(\ell,\gamma)} H_{ji} \right) \left(1 - \sum_{i=1}^{6} n_i^{(\ell,\gamma)} H_{ji} \right) \right)$$
$$- \frac{(1-\varepsilon)}{\varepsilon} N_1 P_1 \left(k^* \sum_{i=1}^{6} n_i^{(\ell,\gamma)} H_{ji} \right);$$
$$\ell = 1, 2, \ldots, s_1, \ \gamma = 1, 2, \ldots, s_2 \tag{25}$$

$$\sum_{i=1}^{6} \frac{dn_i^{(\ell,\gamma)}}{d\tau} H_{ji} = P_1 \left(C_1 \left(\sum_{i=1}^{6} q_i^{(\ell,\gamma)} H_{ji} \right) \left(1 - \sum_{i=1}^{6} n_i^{(\ell,\gamma)} H_{ji} \right) \right)$$
$$- P_1 \left(k^* \sum_{i=1}^{6} n_i^{(\ell,\gamma)} H_{ji} \right);$$
$$\ell = 1, 2, \ldots, s_1, \ \gamma = 1, 2, \ldots, s_2 \tag{26}$$

$$\sum_{i=1}^{6} \frac{dc_i^{(\gamma)}}{d\tau} H_{ji} = \frac{\psi Bi}{Peh_\gamma^2} \sum_{i=1}^{6} c_i^{(\gamma)} \overline{B}_{ji} - \frac{\psi Bi}{h_\gamma} \sum_{i=1}^{6} c_i^{(\gamma)} \overline{A}_{ji}$$
$$- \theta Bi \left(\sum_{i=1}^{6} c_i^{(\gamma)} H_{ji} - \sum_{i=1}^{6} q_i^{(s_1,\gamma)} H_{1i} \right)$$
$$\gamma = 1, 2, \ldots, s_2 \tag{27}$$

B_{ji} and A_{ji} are discretization matrices for second and first order derivatives respectively, in radial domain whereas $\overline{B_{ji}}$ and $\overline{A_{ji}}$ are discretization matrices for second and first order derivatives respectively, in axial domain.

After applying QHCM, for 2 elements in radial domain and varying elements in axial domain '$76s_2$' number of differential equations appears where s_2 is the number of elements in axial domain. This system of differential equations is solved using MATLAB with '$ode15s$' system solver. This subroutine uses backward differentiation formula to discretize the system of ordinary differential equations.

5. Results and discussions

In this section the numerically obtained results are also compared with the published results given in Gupta et al. (2015). However, in Gupta et al. (2015) large number of elements is taken *i.e.* from 5 to 40 elements in radial and axial direction which gives nearly 7000 number of equations to solve according to the formula given in Gupta et al. (2015). Solving such a large system of equations is very difficult and time consuming using MATLAB solver. But in QHCM only 2–8 elements are required which gives nearly 600 equations to solve the model equations.

5.1. Comparison between experimental and model predicted values

Practically it is not possible to vary a single parameter. As bed porosity changes, pore radius of particles, interstitial velocity and permeability vary, which varies axial dispersion coefficient and intraparticle diffusion coefficient which ultimately effects Péclet number and Biot number. In Fig. 4, the combined effect of parameters has been shown graphically through surface plot using experimental values (Arora and Potuček, 2012). It can be easily observed that solution profiles are smooth. From the surface plots one can interpret that the solution profiles also lies within the domain. In Tables 2 and 3 model predicted values are compared to experimental ones and relative error (R.E.) is calculated using the formula:

$$R.E. = \left| \frac{C_{ex} - C_{num}}{C_{ex}} \right| \tag{28}$$

where C_{ex} are the experimental values and C_{num} are the numerical values obtained by finding the solution profiles using QHCM. Numerical values have been compared to the experimental values taken from Arora and Potuček (2012). Numerical values obtained from QHCM have also been compared to the values obtained by Gupta et al. (2015) using cubic spline collocation method (CSCM). Comparison of the values obtained from QHCM and CSCM are presented in Tables 4 and 5. The relative error is found to be of order 10^{-3}. It signifies the validity of the model to a washing cell. This fact authenticates that QHCM is better than technique of CSCM given in Gupta et al. (2015).

5.2. Effect of different parameters

On the basis of results obtained, effect of different parameters on solution profiles has been analyzed and shown graphically through breakthrough curves. Numerical values have been calculated by QHCM using backward differentiation formula with 2×8 elements in radial and axial domain, respectively.
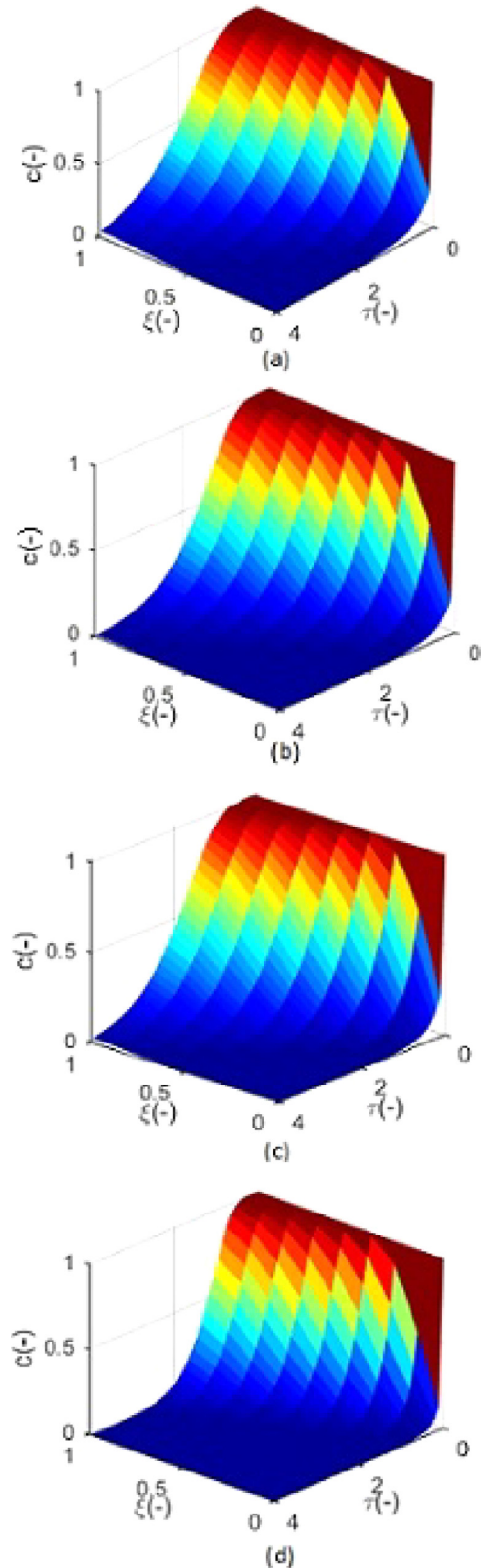

Fig. 4. Graphical view of solution profile through surface plots (a) $Pe = 12.25$, $Bi = 7.4$, $\varepsilon = 0.6898$, (b) $Pe = 12.96$, $Bi = 6.3$, $\varepsilon = 0.8120$, (c) $Pe = 16.92$, $Bi = 7.5$, $\varepsilon = 0.5561$, (d) $Pe = 20.81$, $Bi = 10$, $\varepsilon = 0.6711$.

Table 2
Comparison of present method (QHCM) with the experimental values for Pe =12.25, Bi = 7.4, $\varepsilon = 0.6898$.

Experimental v	Present Method (QHCM)	Relative Error
1.0000×10^0	1.0001×10^0	1.0000×10^{-4}
9.5080×10^{-1}	9.5097×10^{-1}	1.7880×10^{-4}
8.4810×10^{-1}	8.4809×10^{-1}	1.1791×10^{-5}
6.5190×10^{-1}	6.5192×10^{-1}	3.0680×10^{-5}
4.5440×10^{-1}	4.5444×10^{-1}	8.8028×10^{-5}
3.0720×10^{-1}	3.0736×10^{-1}	5.2083×10^{-4}
1.6300×10^{-1}	1.6303×10^{-1}	1.8405×10^{-4}
7.2010×10^{-2}	7.2012×10^{-2}	2.7774×10^{-5}
2.7650×10^{-2}	2.7660×10^{-2}	3.6166×10^{-4}
9.7270×10^{-3}	9.7251×10^{-3}	1.9533×10^{-4}
4.5730×10^{-3}	4.5702×10^{-3}	6.1229×10^{-4}
2.0310×10^{-3}	2.0310×10^{-3}	0
1.1950×10^{-3}	1.1940×10^{-3}	8.3682×10^{-4}
8.1400×10^{-4}	8.1372×10^{-4}	3.4398×10^{-4}
6.0800×10^{-4}	6.0841×10^{-4}	6.7434×10^{-4}

Table 3
Comparison of present method (QHCM) with the experimental values for Pe =16.92, Bi = 7.5, $\varepsilon = 0.5561$.

Experimental Values	Present Method (QHCM)	Relative Error
1.0000×10^0	1.0002×10^0	2.0000×10^{-4}
1.0000×10^0	1.0001×10^0	1.0000×10^{-4}
9.8000×10^{-1}	9.8013×10^{-1}	1.3265×10^{-4}
8.7850×10^{-1}	8.7864×10^{-1}	1.5936×10^{-4}
7.0770×10^{-1}	7.0769×10^{-1}	1.4130×10^{-5}
5.3960×10^{-1}	5.3965×10^{-1}	9.2661×10^{-5}
3.9420×10^{-1}	3.9412×10^{-1}	2.0294×10^{-4}
2.4040×10^{-1}	2.4046×10^{-1}	2.4958×10^{-4}
8.3850×10^{-2}	8.3887×10^{-2}	4.4126×10^{-4}
1.9040×10^{-2}	1.9040×10^{-2}	0
6.5390×10^{-3}	6.5387×10^{-3}	4.5879×10^{-5}
2.6150×10^{-3}	2.6158×10^{-3}	3.0593×10^{-4}
1.4040×10^{-3}	1.4050×10^{-3}	7.1225×10^{-4}
9.3100×10^{-4}	9.3139×10^{-4}	4.1890×10^{-4}
6.7700×10^{-4}	6.7663×10^{-4}	5.4653×10^{-4}

5.2.1. Effect of Péclet number (Pe):

Péclet number is the ratio of advection to dispersion. Being inversely proportional to axial dispersion coefficient, higher Péclet number implies smaller axial dispersion coefficient which in turn implies less back mixing and hence, better removal of impurities adsorbed on particle surface. In Figs. 5 and 6, the effect of Pe is analyzed for different ranges *i.e.* 5–20 and 50–100, respectively. It is observed that for small range of Pe solution profiles takes long time to converge to steady state. This occurs due to large value of axial dispersion coefficient which causes back mixing and as a result long time is required to leach out the impurities adsorbed on particle surface and vice versa. No considerable effect is observed for $Pe > 100$.

5.2.2. Effect of Biot number (Bi):

Biot number represents the mass transfer resistances inside and on the surface of the particle. It is also an important parameter in the process of displacement washing. In Fig. 7 behaviour of solution profiles is shown for different values of Bi. It is observed that for large values of Bi solution profiles converge faster as compare to small values of Bi. It shows that mass transfer rate increases with the increase in Biot number which increases the rate of removal of impurities adsorbed on particle surface and vice versa.

5.2.3. Effect of Bed porosity (ε):

Bed porosity is one of the most perceptive factor which influences the process of displacement washing. As bed porosity increases, permeability increases which results in more removal of solute from intraparticle voids which accelerates the convective mechanism and hence better washing operations can be achieved. This theoretical interpretation is shown in Fig. 8 where the behaviour of solution profiles is shown for varying values of bed porosity.

6. Conclusions

A nonlinear advection dispersion model for packed bed of porous particles has been discretized using quintic Hermite collocation method. Numerical results obtained through QHCM have been compared to the experimental values of Arora and Potuček (2012). The relative error is found to be of order 10^{-3}. Numerical results are also compared to the Gupta et al. (2015) in different perspectives as number of elements to be taken, the relative error according to the mathematical point of view. This fact authenticates the validity and applicability of QHCM. Results are shown in tabular as well as graphical form through which the smoothness of solution profiles can be easily observed. It can be concluded from all the findings that mathematical advection dispersion

Table 4
Comparison of present method (QHCM) with CSCM given in Gupta et al. (2015) for Pe =12.96, Bi = 6.3, $\varepsilon = 0.8120$.

Experimental Values	Present Method (CSCM)	Gupta et al. (2015) (QHCM)	Relative Error (QHCM)	Relative Error (CSCM)
1.0000	1.0001	1.0001	1.0000×10^{-4}	1.0000×10^{-4}
0.9473	0.9472	0.9471	1.0556×10^{-4}	2.1113×10^{-4}
0.8378	0.8377	0.8372	1.1936×10^{-4}	7.1616×10^{-4}
0.7420	0.7421	0.7431	1.3477×10^{-4}	1.4825×10^{-3}
0.6409	0.6409	0.6418	0	1.4043×10^{-3}
0.5483	0.5485	0.5481	3.6476×10^{-4}	3.6476×10^{-4}
0.4300	0.4300	0.4313	0	3.0233×10^{-3}
0.3121	0.3123	0.3135	6.4082×10^{-4}	4.4857×10^{-3}
0.2132	0.2132	0.2119	0	6.0976×10^{-3}
0.1139	0.1139	0.1147	0	7.0237×10^{-3}
0.0576	0.0575	–	1.7000×10^{-3}	–
0.0266	0.0265	–	3.8000×10^{-3}	–
0.0100	0.0100	–	0	–
0.0039	0.0039	–	0	–
0.0016	0.0016	–	0	–

Table 5
Comparison of present method (QHCM) with CSCM given in Gupta et al. (2015) for Pe =20.81, Bi = 10, ε = 0.6711.

| Experimental Values	Present Method (QHCM)	Gupta et al. (2015) (CSCM)	Relative Error (QHCM)	Relative Error (CSCM)
1.0000	1.0001	–	1.0000×10^{-4}	–
0.9900	0.9901	0.9907	1.0101×10^{-4}	7.0707×10^{-4}
0.9385	0.9384	0.9379	1.0655×10^{-4}	6.3932×10^{-4}
0.8169	0.8170	0.8158	1.2241×10^{-4}	1.3466×10^{-3}
0.6743	0.6744	0.6736	1.4830×10^{-4}	1.0381×10^{-3}
0.5335	0.5334	0.5343	1.8744×10^{-4}	1.4995×10^{-3}
0.4560	0.4559	0.4571	2.1930×10^{-4}	2.4123×10^{-3}
0.3556	0.3554	0.3546	5.6243×10^{-4}	2.8121×10^{-3}
0.2685	0.2685	0.2674	0	4.0968×10^{-3}
0.1849	0.1850	0.1891	5.4083×10^{-4}	2.2715×10^{-2}
0.1095	0.1094	0.1056	9.1324×10^{-4}	3.5616×10^{-2}
0.0429	0.0430	–	2.3000×10^{-3}	–
0.0054	0.0054	–	0	–
0.0019	0.0019	–	0	–
0.0005	0.0005	–	0	–
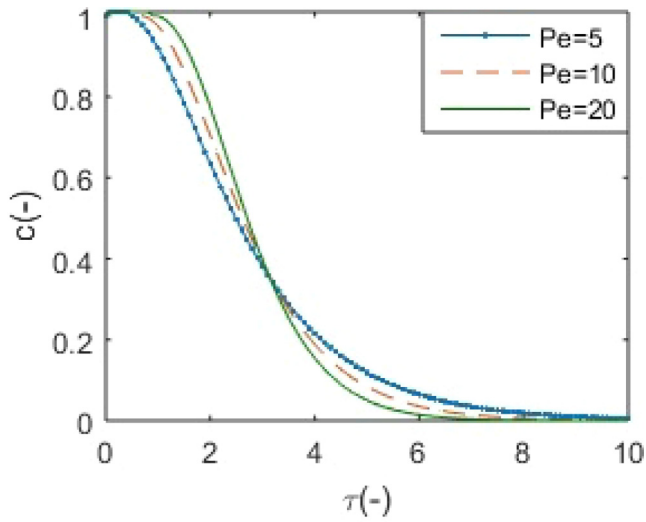
Fig. 5. Effect of solution profiles for different range of $Pe, Bi = 5$, $\varepsilon = 0.6711$ and $\psi = 0.1$.
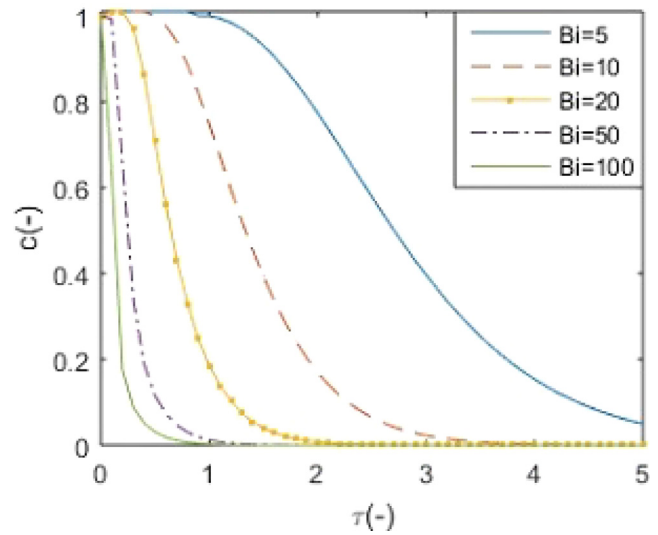

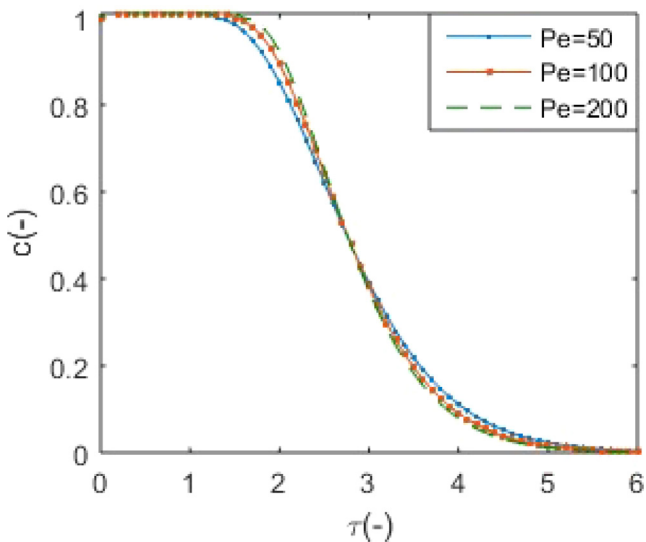**Fig. 7.** Effect of solution profiles for different values of $Bi, Pe = 20$, $\varepsilon = 0.6711$ and $\psi = 0.1$.

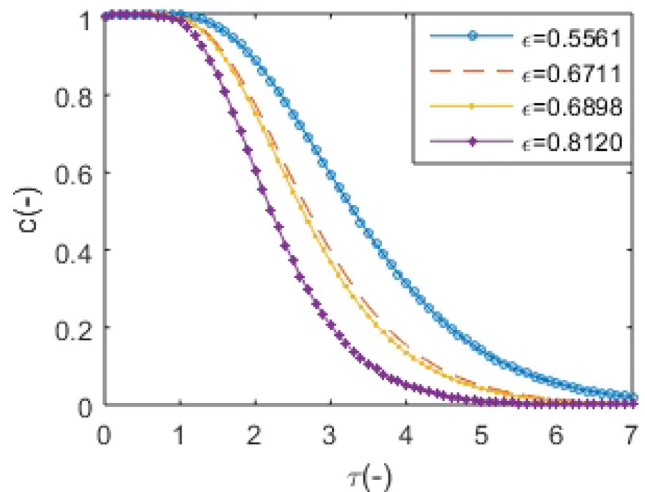**Fig. 6.** Effect of solution profiles for different range of $Pe, Bi = 5$, $\varepsilon = 0.6711$ and $\psi = 0.1$.

Fig. 8. Effect of solution profiles for different values $\varepsilon, Pe = 20$, $\psi = 0.1$ and $Bi = 5$.

model agrees well with the experimental data. Graphical and tabular views of the solution profiles show the efficiency of QHCM.

Acknowledgement

References

Arora, S., Dhaliwal, S.S., Kukreja, V.K., 2006. Simulation of washing of packed bed of porous particles by orthogonal collocation on finite elements. Comput. Chem. Eng. 30, 1054–1060.

Arora, S., Potuček, F., 2012. Verification of mathematical model for displacement washing of kraft pulp fibers. Indian J. Chem. Technol. 19, 140–148.

Arora, S., Kaur, I., 2018. Applications of quintic Hermite collocation with time discretization to singularly perturbed problems. Appl. Math. Comput. 316, 409–421.

Arora, S., Kaur, I., Potuček, F., 2015. Modelling of displacement washing of pulp fibers using the Hermite collocation method. Braz. J. Chem. Eng. 32, 563–575.

Arora, S., Kaur, I., 2016. An efficient scheme for numerical solution of Burgers' equation using quintic Hermite interpolating polynomials. Arabian J. Math 5, 23–34.

Arora, S., Kaur, I., Kumar, H., Kukreja, V.K., 2017. A robust technique of cubic Hermite collocation for solution of two phase non-linear model. J. King Saud Univ. Eng. Sci. 29, 159–165.

Arora, S., Kukreja, V.K., Potuček, F., 2014. Analytic solution of biparameter axial dispersion model. Commun. Appl. Ind. Math. https://doi.org/10.1685/journal.caim.458.

Arora, S., Potuček, F., 2009. Modelling of displacement washing of packed bed of fibers. Braz. J. Chem. Eng. 26, 385–393.

Brenner, H., 1962. The diffusion model of longitudinal mixing in beds of finite length Numerical values. Chem. Eng. Sci. 17, 229–243.

Gupta, B., Kukreja, V.K., Parumasur, N., Singh, P., 2015. Numerical study of a nonlinear diffusion model for washing of packed bed of cylindrical fiber particles. Arab. J. Sci. Eng. 40, 1279–1287.

Neretnieks, I., 1974. A mathematical model for continuous counter current adsorption. Svensk Papperstidning-Nordisk Cellulosa 11, 407–411.

Pellett, G.L., 1966. Longitudinal dispersion, intraparticle diffusion and liquid-phase mass transfer during flow through multiparticle systems. Tappi J. 49, 75–82.

Potuček, F., 1997. Washing of pulp fibre bed. Collect. Czech. Chem. Commun. 62, 626–644.

Raghvan, N.S., Ruthven, D.M., 1983. Numerical simulation of a fixed bed adsorption column by the method of orthogonal collocation. Am. Inst. Chem. Eng. 29, 922–925.

Rosen, J.B., 1952. Kinetics of a fixed bed system for solid diffusion in to spherical particles. J. Chem. Phys. 20, 387–390.

Sherman, W.R., 1964. The movement of a soluble material during the washing of a bed of packed solids. Am. Inst. Chem. Eng. 10, 855–860.